Online Mixed-Integer Optimization in Milliseconds

Dimitris Bertsimas and Bartolomeo Stellato

July 1, 2020

Abstract

We propose a method to solve online mixed-integer optimization (MIO) problems at very high speed using machine learning. By exploiting the repetitive nature of online optimization, we are able to greatly speedup the solution time. Our approach encodes the optimal solution into a small amount of information denoted as *strategy* using the Voice of Optimization framework proposed in [BS20]. In this way the core part of the optimization algorithm becomes a multiclass classification problem which can be solved very quickly. In this work we extend that framework to real-time and high-speed applications focusing on parametric mixed-integer quadratic optimization (MIQO). We propose an extremely fast online optimization algorithm consisting of a feedforward neural network (NN) evaluation and a linear system solution where the matrix has already been factorized. Therefore, this online approach does not require any solver nor iterative algorithm. We show the speed of the proposed method both in terms of total computations required and measured execution time. We estimate the number of floating point operations (flops) required to completely recover the optimal solution as a function of the problem dimensions. Compared to state-of-the-art MIO routines, the online running time of our method is very predictable and can be lower than a single matrix factorization time. We benchmark our method against the state-of-the-art solver Gurobi obtaining from two to three orders of magnitude speedups on examples from fuel cell energy management, sparse portfolio optimization and motion planning with obstacle avoidance.

1

1 Introduction

Mixed-integer optimization (MIO) has become a powerful tool for modeling and solving real-world decision making problems; see [JLN+10]. While most MIO problems are $\mathcal{NP}$-hard and thus considered intractable, we are now able to solve instances with complexity and dimensions that were unthinkable just a decade ago. In [Bix10] the authors analyzed the impressive rate at which the computational power of MIO grew in the last 25 years providing over a trillion times speedups. This remarkable progress is due to both algorithmic and hardware improvements. Despite these advances, MIO is still considered harder to solve than convex optimization and, therefore, it is more rarely applied to online settings.

Online optimization differs from general optimization by requiring on the one hand computing times strictly within the application limits and on the other hand limited computing resources. Fortunately, while online optimization problems are not the same between each solve, only some parameters vary and the structure remains unchanged. For this reason, online optimization falls into the broader class of parametric optimization where we can greatly exploit the repetitive structure of the problem instances. In particular, there is a significant amount of data that we can reuse from the previous solutions.

In a recent work [BS20], the authors constructed a framework to predict and interpret the optimal solution of parametric optimization problems using machine learning. By encoding the optimal solution into a small amount of information denoted as *strategy*, the authors convert the solution algorithm into a multiclass classification problem. Using interpretable machine learning predictors such as optimal classification trees (OCTs), Bertsimas and Stellato were able to understand and interpret how the problem parameters affect the optimal solutions. Therefore they were able to give optimization a *voice* that the practitioner can understand.

In this paper we extend the framework from [BS20] to online optimization focusing on speed and real-time applications instead of interpretability. This allows us to obtain an end-to-end approach to solve mixed-integer optimization problems online without the need of any solver nor linear system factorization. The online solution is extremely fast and can be carried out less than a millisecond reducing the online computation time by more than two orders of magnitude compared to state-of-the-art algorithms.

1.1 Contributions

In this work, by exploiting the structure of mixed-integer quadratic optimization (MIQO) problems, we derive a very fast online solution algorithm where the whole optimization is reduced to a neural network (NN) prediction and a single linear system solution. Even though our approach shares the same framework as [BS20], it is substantially different in the focus and the final algorithm. The focus is primarily speed and online optimization applications and not interpretability as in [BS20]. This is why for our predictions we use non interpretable, but very fast, methods such as NNs. Furthermore, our final algorithm does not involve any convex optimization problem solution as in [BS20]. Instead, we just apply simple matrix-vector multiplications. Our specific contributions include:

1. We focus on the class of MIQO instead of dealing with general mixed-integer convex optimization (MICO) as in [BS20]. This allows us to replace the final step to recover the solution with a simple linear system solution based on the KKT optimality conditions of the reduced problem. Therefore, the whole procedure does not require any solver to run compared to [BS20].

2. To reduce the number of strategies in larger examples, we reassign the samples to a lower number of selected strategies so that the average suboptimality and infeasibility do not increase above certain tolerances. We define this step as "strategy pruning" and formulate it as a large-scale mixed-integer linear optimization (MILO). To provide solutions in reasonable times, we develop an approximation algorithm that reassings the training samples according to the strategies appearing most often.

3. In several practical applications of MIQO, the KKT matrix of the reduced problem does not change with the parameters. In this work we factorize it offline and cache the factorization for all the possible solution strategies appearing in the data. By doing so, our online solution step becomes a sequence of simple forward-backward substitutions that we can carry out very efficiently. Hence, with the offline factorization, our overall online procedure does not even require a single matrix factorization. Compared to [BS20], this further simplifies the online solution step.

4. After the algorithm simplifications, we derive the precise complexity of the overall algorithm in terms of floating point operations (flops) which does not depend on the problem parameters values. This makes the execution time predictable and reliable compared to branch-and-bound (B&B) algorithms which often get stuck in the tree search procedure.

5. We benchmark our method against state-of-the-art MIQO solver Gurobi on sparse portfolio trading, fuel battery management and motion planning examples. Thanks to the strategy pruning, we obtain between few hundreds to less than 10,000 strategies for all the examples. This allows to achieve high quality strategy predictions in terms of suboptimality and infeasibility. In particular, the average suboptimality is comparable to the one from Gurobi heuristics and infeasibility is always within acceptable values for the applications considered. Timing comparisons show up to three orders of magnitude speedups compared to both Gurobi global optimizer and Gurobi heuristics. The worst-case solution time of our method is also up to three orders of magnitude smaller than the one obtained with B&B schemes, enabling real-time implementations in milliseconds.

1.2   Outline

The structure of the paper is as follows. In Section 2, we review recent work on machine learning for optimization outlining the relationships and limitations of other methods compared to approach presented in this work. In addition, we outline the recent developments in high-speed online optimization and the limited advances that appeared so far for MIO. In Section 3, we introduce the Voice of Optimization framework from [BS20] for general MIO describing the concept of solution *strategy*. In Section 4, we describe the strategies selection problem as a multiclass classification problem and propose the NN architecture used in the prediction phase. We also introduce a strategy pruning scheme to reduce the number of strategies. Section 5 describes the computation savings that we can obtain with problem with a specific structure such as MIQO and the worst-case complexity in terms of number of flops. In Section 6, we describe the overall algorithm with the implementation details. Benchmarks comparing our method to the state-of-the-art solver Gurobi examples with realistic data appear in Section 7.

2 Related Work

2.1 Machine learning for optimization

Recently the operations research community started to focus on systematic ways to analyze and solve combinatorial optimization problems with the help of machine learning. For an extensive review on the topic we refer the reader to [BLP18].

Machine learning has so far helped optimization in two directions. The first one investigates heuristics to improve solution algorithms. Iterative routines deal with repeated decisions where the answers are based on expert knowledge and manual tuning. A common example is branching heuristics in B&B algorithms. In general these rules are hand tuned and encoded into the solvers. However, the hand tuning can be hard and is in general suboptimal, especially with complex decisions such as B&B algorithm behavior. To overcome these limitations in [KBS+16] the authors learn the branching rules without the need of expert knowledge showing comparable or even better performance than hand-tuned algorithms. Other promising results using ExtraTrees to learn branching rules appeared in [ALW17]. We refer the reader to [LZ17] for a review on the intersection of machine learning and branching.

Another example appears in [BLZ18] where the authors investigate whether it is faster to solve MIQOs directly or as second-order cone optimization (SOCO) problems by linearizing the cost function. This problem becomes a classification problem that offers an advantage based on previous data compared to how the decision is heuristically made inside off-the-shelf solvers.

The second direction poses combinatorial problems as control tasks that we can analyze under the reinforcement learning framework [SB18]. This is applicable to problems with multistage decisions such as network problems or knapsack-like problems. [DKZ+17] learn the heuristic criteria for stagewise decisions in problems over graphs. In other words, they build a greedy heuristic framework, where they learn the node selection policy using a specialized neural network able to process graphs of any size [DDS16]. For every node, the authors feed a graph representation of the problem to the network and they receive an action-value pair suggesting the next node to select in the optimal path.

Even though these two directions introduce optimization to the benefits

of machine learning and show promising results, they do not consider the parametric nature of problems solved in real-world applications. We often solve the same problem formulation with slightly varying parameters several times generating a large amount of data describing how the parameters affect the solution.

Recently, this idea was used to devise a sampling scheme to collect all the optimal active sets appearing from the problem parameters in continuous convex optimization [MRN19]. While this approach is promising, it evaluates online all the combinations of the collected active sets without predicting the optimal ones using machine learning. Another related work appeared in [KKK19] where the authors warm-start online active set solvers using the predicted active sets from a machine learning framework. However, they do not provide probabilistic guarantees for that method and their sampling scheme is tailored to their specific application of quadratic optimization (QO) for model predictive control (MPC).

In our work, we propose a new method that exploits the amount of data generated by parametric problems to solve MIO online at high speed. In particular we study how efficient we can make the computations using a combination of machine learning and optimization. To the authors knowledge this is the first time machine learning is used to both reduce and make more consistent the solution time of MIO algorithms.

2.2 Online optimization

Applications of online optimization span a wide variety of fields including scheduling [CaPM10], supply chain management [YG08], hybrid model predictive control [BM99], signal decoding [DCB00].

Embedded optimization.   Over the last decade there has been a significant attention from the community for tools for generating custom solvers for online parametric programs. CVXGEN [MB12] is a code generation software for parametric QO that produces a fast and reliable solver. However, its code size grows dramatically with the problem dimensions and it is not applicable to large problems. More recently, the OSQP solver [SBG$^+$20] showed remarkable performance with a light first-order method greatly exploiting the structure of parametric programs to save computation time. The OSQP authors also proposed an optimized version for embedded applications in [BSM$^+$17].

Other solvers that can exploit the structure of parametric programs in online settings include qpOASES [FKP+14] for QO and ECOS [DCB13] for SOCO.

Parametric MIQOs. However, all these approaches focus on continuous convex problems with no integer variables such as QO. This is because of two main reasons. On the one hand, mixed-integer optimization algorithms are far more complicated to implement than convex optimization ones since they feature a massive amount of heuristics and preprocessing. This is why there is still a huge gap in performance between open and commercial solvers for MIO. On the other hand, for many online applications the solution time required to solve MIO problems is still not compatible with the amount of time allowed. An example is hybrid MPC where depending on the system dynamics, we have to solve MIO problems online in fractions of a second. Explicit hybrid MPC tackles this issue by precomputing offline the entire mapping between the parameter space to the optimal solution [BMDP02]. However, the memory required for storing such solutions grows exponentially with the problem dimensions and this approach easily becomes intractable.

Suboptimal heuristics. Other approaches solve these problems only suboptimally using heuristics to deal with insufficient time to compute the globally optimal solution. Examples include the Feasibility Pump heuristic [FGL05] that iteratively solves linear optimization (LO) subproblems and rounds their solutions until it finds a feasible solution for the original MIO problem. Another heuristic works by integrating the alternating direction method of multipliers (ADMM) [DTB18] with rounding steps to obtain integer feasible solutions for the original problem. The downside of these heuristics is that they do not exploit the large amount of data that we gain by solving the parametric problems over and over again in online settings.

Warm-starting. In order to speedup subsequent solves, several works focus on warm-starting B&B algorithms [GHW15, RG06]. However, there can be three possible reasons for which significant solution time speedups cannot be achieved. First, previous solutions can be infeasible for the current problem and, therefore, not useful to create bounds to quickly prune branches in the B&B tree. Second, many commercial solvers apply fast heuristics that can quickly obtain good feasible solutions. In case these solutions are as good or better than the provided one, warm-starting does not bring any

7

benefit; see, *e.g.*, [GO20, `Start` variable attribute]. Third, in B&B algorithms the vast majority of time is usually spent to prove optimality and we are not able to significantly reduce it with a warm-started solution [GHW15, Section 4]. Instead of providing only the previous optimal solution, we can pass the previous B&B tree and adapt the nodes according to parameter changes [MT19]. This technique can sometimes greatly reduce the number of QOs solved. However, it still requires a B&B algorithm to complete, which might be too slow in fast real-time settings.

Value function approximations. Parametric MIQO have also been studied in terms of how the optimal cost changes with the parameters, *i.e.*, the value function. The authors of [HR14] propose an iterative scheme to dynamically generate points to construct approximations of the value function with applications to stochastic integer and bilevel integer optimization problems. Constructing value functions to solve stochastic MIO has been studied also in [TPS19, TPS13]. Our approach also tries to map the parameters to the optimizer output but with two main differences: first it relies on data, second it encodes the optimal solution and not the value function.

Our approach. Despite all these efforts in solving MIO online, there is still a significant gap between the solution time and the real-time constraints of many applications. In this work we propose an alternative approach that exploits data coming from previous problem solutions with high-performance MIO solvers to reduce the online computation time making it possible to apply MIO to online problems that were not approachable before. The aproach proposed in this paper has already been applied to control problems in robotics in [CCS+20] by exploiting the application-specific structure of the constraints.

3   The Voice of Optimization

In this section we introduce the idea of the optimal strategy following the same framework first introduced in [BS20]. Given a parameter $\theta \in \mathbf{R}^p$, we define a *strategy $s(\theta)$* as the complete information needed to efficiently recover the optimal solution of an optimization problem.

Consider the mixed-integer optimization problem

$$
\begin{array}{ll}
\text{minimize} & f(\theta, x) \\
\text{subject to} & g(\theta, x) \le 0, \\
& x_{\mathcal{I}} \in \mathbf{Z}^d,
\end{array}
\tag{1}
$$

where $x \in \mathbf{R}^n$ is the decision variable and $\theta \in \mathbf{R}^p$ defines the parameters affecting the problem. We denote the cost as $f : \mathbf{R}^p \times \mathbf{R}^n \to \mathbf{R}$ and the constraints as $g : \mathbf{R}^p \times \mathbf{R}^n \to \mathbf{R}^m$. The vector $x^\star(\theta)$ denotes the optimal solution and $f(\theta, x^\star(\theta))$ the optimal cost function value given the parameter θ.

Optimal strategy. We now define the optimal strategy as the set of tight constraints together with the value of integer variables at the optimal solution. We denote the *tight constraints* $\mathcal{T}(\theta)$ as constraints that are equalities at optimality,

$$
\mathcal{T}(\theta) = \{i \in \{1, \ldots, m\} \mid g_i(\theta, x^\star(\theta)) = 0\}.
\tag{2}
$$

Hence, given the $\mathcal{T}(\theta)$ all the other constraints are redundant for the original problem.

If we assume linear independence constraint qualification (LICQ), the number of tight constraints is at most n because the tight constraints gradients at the solution $\nabla g_i(\theta, x^\star(\theta)) \in \mathbf{R}^n$, $i \in \mathcal{T}(\theta)$ are linearly independent [NW06, Section 12.2], . When LICQ does not hold, the number of tight constraints can be more than the number of decision variables, *i.e.*, $|\mathcal{T}(\theta)| > n$. However, in practice the number of tight constraints is significantly lower than the number of constraints m, even for degenerate problems. This means that for many applications where the number of constraints is larger than the number of variables, by knowing $\mathcal{T}(\theta)$ we can to neglect a large number of redundant constraints at the optimal solution.

When some of the components of x are integer, we cannot easily compute the optimal solution by knowing only $\mathcal{T}(\theta)$. This is because the solution retrieval would involve a MIO problem to identify the integer components of x. However, after fixing the integer components to their optimal values $x^\star_{\mathcal{I}}(\theta)$, the tight constraints allow us to efficiently compute the optimal solution. Hence the strategy identifying the optimal solution is a tuple containing the index of tight constraints at optimality and the optimal value of the integer variables, *i.e.*, $s(\theta) = (\mathcal{T}(\theta), x^\star_{\mathcal{I}}(\theta))$.

Solution method. Given the optimal strategy, solving (1) corresponds to solving the following optimization problem

$$\begin{array}{ll} \text{minimize} & f(\theta, x) \\ \text{subject to} & g_i(\theta, x) \leq 0, \quad \forall i \in \mathcal{T}(\theta) \\ & x_\mathcal{I} = x_\mathcal{I}^\star(\theta), \end{array} \quad (3)$$

Solving (3) is much easier than (1) because it is continuous, convex and has a smaller number of constraints. Note that, we cannot in general enforce $g_i(\theta, x) = 0$ for the tight constraints because it would make (3) nonconvex. However, we can enforce equalities when g_i are linear in x [BV04]. Since it is a very fast and direct step, we will denote it as *solution decoding*. In Section 5 we describe the details of how to exploit the structure of (3) and compute the optimal solution online at very high speeds.

4 Machine Learning

In this section, we describe how we learn the mapping from the parameters θ to the optimal strategies $s(\theta)$. In this way, we can replace the hardest part of the optimization routine by a prediction step in a multiclass classification problem where each strategy is a class label.

4.1 Multiclass Classifier

Our classification problem features data points $(\theta_i, s_i), \ i = 1, \ldots, N$ where $\theta_i \in \mathbf{R}^p$ are the parameters and $s_i \in \mathcal{S}$ the corresponding labels identifying the optimal strategies. Set $\mathcal{S}$ is the set of strategies of cardinality $|\mathcal{S}| = M$. Our goal is to predict $\hat{s}_i$ so that it is as close as possible to the true s_i given sample θ_i.

We solve the classification task using NNs. NNs have recently become the most popular machine learning method radically changing the way we classify in fields such as computer vision [KSH12], speech recognition [HDY+12], autonomous driving [BDTD+16], and reinforcement learning [SSS+17].

In this work we choose feedforward neural networks because they offer a good balance between simplicity and accuracy without the need of more advanced architectures such as convolutional or recurrent NNs [LBH15].

Architecture. We deploy a similar architecture as in [BS20] consisting of L layers defining a composition of functions of the form

$$\hat{s} = h_L(h_{L-1}(\ldots h_1(\theta))),$$

where each layer consists of

$$y_l = h_l(y_{l-1}) = \sigma_l(W_l y_{l-1} + b_l), \quad i = 1, \ldots, L, \tag{4}$$

where $y_l \in \mathbf{R}^{n_l}$. We define the *input* layer as $l = 1$ and the *output* layer as $l = L$ so that $y_0 = \theta$ and $y_L = \hat{s}$.

Each layer performs an affine transformation with parameters $W_l \in \mathbf{R}^{n_l \times n_{l-1}}$ and $b_l \in \mathbf{R}^{n_l}$. In addition, it includes an activation function $\sigma : \mathbf{R}^{n_l} \to \mathbf{R}^{n_l}$ to model nonlinearities. Inner layers feature a rectified linear unit (ReLU) defined as

$$\sigma_l(x) = \max(x, 0), \quad l = 1, \ldots, L - 1,$$

where the max operator is intended elementwise. The ReLU operator has become popular because it promotes sparsity to the model outputting 0 for the negative components of x and because it does not experience vanishing gradient issues typical in sigmoid functions [GBC16].

The output layer features a softmax activation function $\sigma_L(x) \in \mathbf{R}^M$ to provide a normalized ranking between the strategies and quantify how likely they are to be the correct one. Softmax activation functions are very common in multiclass classificaiton because of their smoothness and the probabilistic interpretation of their output as the relative importance between classes [GBC16, Section 6.2.2.3]. We can write the output layer as

$$(\sigma_L(x))_j = \frac{e^{x_j}}{\sum_{j=1}^{M} e^{x_j}},$$

where $0 \le \sigma_L(x) \le 1$ because of the nonnegativity of the exponential functon and the normalization factor.

Learning. In order to define a proper cost function and train the network we rewrite the labels as a one-hot encoding, *i.e.*, $s_i \in \mathbf{R}^M$ where M is the total number of classes and all the elements of s_i are 0 except the one corresponding

to the class which is 1. Then we define a smooth cost function, *i.e.*, the cross-entropy loss for which gradient descent-like algorithms work well

$$\mathcal{L}_{\mathrm{NN}} = \sum_{i=1}^{N} -s_i^T \log(\hat{s}_i),$$

where log is intended elementwise. This loss $\mathcal{L}$ can also be interpreted as the distance between the predicted probability density of the labels and to the true one. The training step consists of applying the classic stochastic gradient descent with the derivatives of the cost function obtained using the back-propagation rule.

Online predictions. After we complete the model training, we can predict the optimal strategy given θ. However, the model can never be perfect and there can be situations where the prediction is not correct. To overcome these possible limitations, instead of considering only the best class predicted by the NN we pick the k most-likely classes. Afterwards, we can evaluate in parallel their feasibility and objective value and pick the feasible one with the best objective.

4.2 Strategies Exploration

It is difficult to estimate the amount of data required to accurately learn the classifier for problem (1). In particular, given N independent samples $\Theta_N = \{\theta_1, \ldots, \theta_N\}$ drawn from an unknown discrete distribution we find M different strategies $\mathcal{S}(\Theta_N) = \{s_1, \ldots, s_M\}$. How likely is it to encounter new strategies in the next sample θ_{N+1}? Following the approach in [BS20], we use the same algorithm to iteratively sample and estimate the probability of finding unseen strategies

$$\mathbf{P}(s(\theta_{N+1}) \notin \mathcal{S}(\Theta_N)),$$

using the Good-Turing estimator [Goo53]. Given a desired probability guarantee $\epsilon > 0$ and confidence interval $\beta > 0$, the algorithm terminates when a bound on the probability of finding new strategies falls below ϵ.

4.3 Strategy Pruning

For some problems, the number of strategies M can quickly grow, thereby making the multiclass classification task very difficult. Fortunately, different

strategies are often redundant because they correspond to multiple global optima and we can select only the relevant strategies to apply.

Mixed-integer linear optimization modelling. For every sample i and strategy j, we can compute the solution to the reduced problem (3) obtaining an objective value f_{ij}. If the reduced problem is infeasible, we set $f_{ij} = \infty$. To simplify the notation, we refer to $\bar{f}_i = f(\theta_i, x^\star(\theta_i))$ as the optimal objective value for sample θ_i. We model the sample i to strategy j assignments with variables $x_{ij} \in \{0,1\}$. Variables $p_j \in \{0,1\}$ describe if strategy j is chosen in the pruning. The objective is to minimize the number of strategies selected such that the cost relative cost degradation for each sample i is less than a tolerance ϵ. The pruning problem can be formulated as the following MILO,

$$
\begin{aligned}
\text{minimize} \quad & \textstyle\sum_{j=1}^{M} p_j \\
\text{subject to} \quad & \textstyle\sum_{j=1}^{M} f_{ij} z_{ij} \le \bar{f}_i + \epsilon \left| \bar{f}_i \right|, \quad i = 1, \ldots, N \\
& \textstyle\sum_{j=1}^{M} z_{ij} = 1, \quad i = 1, \ldots, N, \\
& \textstyle\sum_{i=1}^{N} z_{ij} \le p_j, \quad j = 1, \ldots, M, \\
& p \in \{0,1\}^M, \quad z \in \{0,1\}^{N \times M},
\end{aligned}
\tag{5}
$$

where $|\cdot|$ is the absolute value. Unfortunately, it is very costly to construct problem (5) because it involves computing f_{ij} for every combination of samples and strategies. For example, if we have 100,000 samples and 2,000 strategies, we need to solve 200,000,000 reduced problems which can be very challenging, even in the specialized cases from Section 5. In addition, despite recent advances of MILO solvers, (5) with millions of binary variables are often intractable. Therefore, we implement a simpler pruning technique.

Frequency-based heuristic. In most cases, the majority of the samples is assigned to a few strategies and the rest of the strategies appears very rarely. Therefore, if we select the most frequent strategies, we cover the majority of the samples. In this way we have to reassign only a small portion of the samples to the selected strategies without having to compute f_{ij} for every sample-strategy combination. The whole procedure is outlined in Algorithm 2. Given $\alpha > 0$, the function SELECTFREQUENTSTRATEGIES in Algorithm 1 selects the most frequent strategies $\mathcal{S}_\alpha$ appearing in at least $1-\alpha$ fraction of samples. Then, the algorithm selects the discarded samples Θ_d

---
Algorithm 1 (SELECTFREQUENTSTRATEGIES) Select most frequent strategies that are assigned to at least $1 - \alpha$ fraction of samples.

> **input** $\alpha, \{s(\theta_i)\}_{i=1}^{N}, \mathcal{S}$
> **output** $\mathcal{S}_\alpha$
> $t \leftarrow 0, \quad \mathcal{S}_\alpha \leftarrow \emptyset$
> **for** $s \in \mathcal{S}$ **do**
> $q_s \leftarrow |\{s(\theta_i) = s, \quad i = 1, \dots, N\}|$ ▷ Compute strategy occurrences.
> $q_{\text{sorted}} \leftarrow \text{REVERSEARGSORT}(q)$ ▷ Sort occurrences in decreasing order.
> **for** $\ell \in q_{\text{sorted}}$ **do**
> $t \leftarrow t + \ell$ ▷ Update number of samples.
> $\mathcal{S}_\alpha \leftarrow \mathcal{S}_\alpha \cup \{\ell\}$
>   **if** $t > \lceil (1 - \alpha)N \rceil$ **then break**
---

that were not assigned to any strategy in $\mathcal{S}_\alpha$. These samples are then reassigned by comparing their cost f_{ij} with every selected strategy in $\mathcal{S}_\alpha$. If there is at least a sample for which the best reassigned strategy cost f_i is above the tolerance, *i.e.*, $f_i > \bar{f}_i + c |\bar{f}_i|$, then α is reduced to $\alpha/2$ to account for more strategies and fewer discarded sample and the iterations are repeated. Otherwise, we found a strategy pruning and samples assignment satisfying tolerance ϵ and the algorithm terminates. If we reach the maximum number of iterations, it means that there is no feasible assignment given the specified tolerance and the last value of fraction of discarded samples α. Compared to solving problem (5), this method relies on the samples-strategy computation of just a small portion of discarded samples. In addition, there is no need to solve any large-scale MILO, which makes it much more scalable to large settings. The downside of this heuristic approach is that the best strategy assignment uses the most frequent strategies, which might not always be the optimal one. However, for small problems where the MILO is solvable, the heuristic solution always gives similar number of pruned strategies as MILO while always satisfying, by construction, the cost function degradation constraint.

5 High-Speed Online Optimization

Thanks to the learned predictor, our method offers great computational savings compared to solving each problem instance from scratch. In ad-

---

Algorithm 2 Prune strategies while keeping feasibility and low suboptimality

---

   input $\{(\theta_i, s(\theta_i))\}_1^N, \mathcal{S}$
   output $\mathcal{S}$
   $\alpha \leftarrow 0.05$
   for it $= 1, \ldots, \max_{\text{it}}$ **do**
      $\mathcal{S}_\alpha \leftarrow \text{SELECTFREQUENTSTRATEGIES}(\alpha, \{s(\theta_i)\}_{i=1}^N, \mathcal{S})$
      $\Theta_d \leftarrow \{\theta_i \mid s(\theta_i) \notin \mathcal{S}\}$ ▷ Select discarded samples
      for $\theta_i \in \Theta_d$ **do**
         for $s_j \in \mathcal{S}_\alpha$ **do**
            $f_{ij} \leftarrow$ Solve (3)   ▷ Compute sample-strategy pairs
         $f_i \leftarrow \min_j(f_{ij})$ ▷ Reassign sample i to best strategy
         if $f_i > \bar{f}_i + \epsilon |\bar{f}_i|$ **then**   ▷ Suboptimality condition not satisfied
            break
      $\alpha \leftarrow \alpha/2$
   return $\mathcal{S}$

---

dition, when the problem offers a specific structure, we can gain even further speedups and replace the whole optimizer with a linear system solution.

Two major challenges in optimization. By using our previous solutions, the learned predictor maps new parameters θ to the optimal strategy replacing two of the arguably hardest tasks in numerical optimization algorithms:

Tight constraints. Identifying the tight constraints at the optimal solution is in general a hard task because of the combinatorial complexity to search over all the possible combinations of constraints. For this reason the worst-case complexity active-set methods (also called simplex methods for LO) is exponential in the number of constraints [BT97].

Integer variables. It is well known that finding the optimal solution of mixed-integer programs is $\mathcal{NP}$-hard [BW05]. Hence, solving problem (1) online might require a prohibitive computation time because of the combinatorial complexity of computing the optimal values of the integer variables.

We solve both these issues by evaluating our predictor that outputs the optimal strategy $s(\theta)$, *i.e.*, the tight constraints at optimality $\mathcal{T}(\theta)$ and the value

of the integer variables $x_{\mathcal{I}}^{\star}(\theta)$. After evaluating the predictor, computing the optimal solution consists of solving (3) which we can achieve much more efficiently than solving (1), especially in case of special structure.

Special structure. When g is a linear function in x we can directly consider the tight constraints as equalities in (3) without losing convexity. In these cases (3) becomes a convex equality constrained problem that can be solved via Newton's method [BV04, Section 10.2]. We can further simplify the online solution in special cases such as MIQO (and also MILO) of the form

$$
\begin{aligned}
& \text{minimize} && (1/2)x^T P x + q^T x + r \\
& \text{subject to} && Ax \le b \\
& && x_{\mathcal{I}} \in \mathbf{Z}^d,
\end{aligned}
\tag{6}
$$

with cost $P \in \mathbf{S}_+^n$, $q \in \mathbf{R}^n$, $r \in \mathbf{R}$ and constraints $A \in \mathbf{R}^{m \times n}$ and $b \in \mathbf{R}^m$. We omitted the dependency of the problem data on θ for ease of notation. Given the optimal strategy $s(\theta) = (\mathcal{T}(\theta), x_{\mathcal{I}}^{\star}(\theta))$, computing the optimal solution to (6) corresponds to solving the following reduced problem from (3)

$$
\begin{aligned}
& \text{minimize} && (1/2)x^T P x + q^T x + r \\
& \text{subject to} && A_{\mathcal{T}(\theta)} x = b_{\mathcal{T}(\theta)} \\
& && x_{\mathcal{I}} = x_{\mathcal{I}}^{\star}(\theta).
\end{aligned}
\tag{7}
$$

Since it is an equality constrained QO, we can compute the optimal solution by solving the linear system defined by its KKT conditions [BV04, Section 10.1.1]

$$
\begin{bmatrix} P & A_{\mathcal{T}(\theta)}^T & I_{\mathcal{I}}^T \\ A_{\mathcal{T}(\theta)} & & 0 \\ I_{\mathcal{I}} & \end{bmatrix} \begin{bmatrix} x \\ \nu \end{bmatrix} = \begin{bmatrix} -q \\ b_{\mathcal{T}(\theta)} \\ x_{\mathcal{I}}^{\star}(\theta) \end{bmatrix}.
\tag{8}
$$

Matrix I is the identity matrix. Vectors or matrices with a subscript index set identify only the rows corresponding to the indices in that set. ν are the dual variables of the reduced continuous problem. The dimensions of the KKT matrix are $q \times q$ where

$$
q = n + |\mathcal{T}(\theta)| + d.
\tag{9}
$$

We can apply the same method to MILO by setting $P = 0$. In case no integer variables are present $(d = 0)$, the strategy identifies only the tight constraints and the dimension of the linear system (8) reduces to $n + |\mathcal{T}(\theta)|$.

16

5.1 The Efficient Solution Computation

In case of MIQO, solving the linear system (8) corresponds to computing the solution to (6). Let us analyze the components involved in the online computations to further optimize the solution time.

Linear system solution. The linear system (8) is sparse and symmetric and we can solve it with both direct methods and indirect methods. Regarding direct methods, we compute a sparse permuted LDL^T factorization [Dav06] of the KKT matrix where L is a square lower triangular matrix and D a diagonal matrix both with dimensions $q \times q$. The factorization step requires $O(q^3)$ number of flops which can be expensive for large systems. After the factorization, the solution consists only in forward-backward solves which can be evaluated very efficiently and in parallel with complexity $O(q^2)$. Alternatively, when the system is very large we can use an indirect method such as MINRES [PS82] to iteratively approximate the solution by using simple matrix-vector multiplications at each step with complexity q^2. Note that indirect methods while more amenable for large problems, can suffer from bad scaling of the matrix data, requiring many steps before convergence.

Matrix caching. In several cases θ does not affect the matrices P and A in (6). In other words, θ enters only in the linear part of the cost and the right hand side of the constraints and does not affect the KKT matrix in (8). This means that, since we know all the strategies that appeared in the training phase, we can factor each of the KKT matrices and store the factors L and D offline. Therefore, whenever we predict the strategy related to a new parameter θ, we can just perform forward-backward solves to obtain the optimal solution without having to perform a new factorization. This step requires $O(q^2)$ flops – an order of magnitude less than factorizing the matrix.

Parallel strategy evaluation. In Section 4.1 we explained how we transform the strategy selection into a multiclass classification problem. Since we have the ability to compare the quality of different strategies in terms of optimality and feasibility, online we choose the k most likely strategies from the predictor output and we compare their performance. Since the comparison is completely independent between the candidate strategies, we can perform it in parallel saving additional computation time.

5.2 Online Complexity

We now measure the online complexity of the proposed approach in terms of flops. The first step consists in evaluating the neural network with L layers. As shown in (4), each layer consists in a matrix-vector multiplication and additions $W_l y_{l-1} + b_l$ which has order $O(n_l n_{l-1})$ operations [BV04, Section C.1.2]. The ReLU step in the layer does not involve any flop since it is a simple truncation of the non positive components of the layer input. Summing these operations over all the layers, the complexity of evaluating the network becomes

$$O(n_1 n_p + n_2 n_1 + \cdots + n_M n_{L-1}) = O(n_M n_{L-1}),$$

where p is the dimension of the parameter θ and we assume that the number of strategies M is larger than the dimension of any layer. Note that the final softmax layer, while being very useful in the training phase and in its interpretation as likelihood for each class, is unnecessary in the online evaluation since we just need to rank the best strategies.

After the neural network evaluation we can decode the optimal solution by solving the KKT linear system (8) of dimension defined in (9). Since we already factorized it, the online computations are just simple forward-backward substitutions as discussed in Section 5.1. Therefore, the flops required to solve the linear system are

$$O((n + |\mathcal{T}(\theta)| + d)^2).$$

This dimension is in general much smaller than the number of constraints m and mostly depends only on the problem variables. In addition the KKT matrix (8) is sparse and if the factorization matrices are sparse as well, we could further reduce the flops required.

The overall complexity of the complete MIQO online solution taking into account both NN prediction and solution decoding becomes

$$O(n_M n_{L-1} + (n + |\mathcal{T}(\theta)| + d)^2), \tag{10}$$

which does not depend on the cube of any of the problem dimensions. This means that with dense matrices, our method is asymptotically cheaper than factorizing a single linear system since that operation would scale with the cube of its input data. For sparse matrices, we can make similar considerations based on the number of nonzero elements instead of the dimensions [Dav06].

Despite these high-speed considerations on the number of operations required, it is very important to remark the reliability of the computation time required by our approach. The execution time of B&B algorithms greatly depends on how the solution search tree is analyzed and pruned. This can vary significantly when problem parameters change making the whole online optimization procedure unreliable in real-time applications. On the contrary, our method offers a fixed number of operations which we evaluate every time we encounter a new parameter.

6   Machine Learning Optimizer

Our implementation extends the software tool machine learning optimizer (MLOPT) from [BS20] which is implemented in Python and integrated with CVXPY [DB16] to model the optimization problems. MLOPT is available at

https://github.com/bstellato/mlopt.

To speedup the repetitive canonicalizations of parametric MIQO we use the disciplined parametric program (DPP) language introduced in CVXPY 1.1 [AAB$^+$19]. In this way, independently from how the parameters affect the data, constructing a new problem instance given a new θ_i consists of a matrix-vector multiplication. MLOPT relies on the Gurobi Optimizer [GO20] to solve the problems in the training phase with high accuracy and identify the tight constraints.

After MLOPT collects the strategies, we apply Algorithm 2 to select the most frequent ones and reassign the samples accordingly. This process is performed in parallel over multiple cores to minimize the independent evaluations. Then, MLOPT passes the data to PyTorch [PGC$^+$17] using Pytorch-Lightning [Fal19] library to define the architecture and train the NN to classify the strategies. We split the training data into 80 % training and 20 % validation. We tune the neural network depth, width, learning rate, batch size, number of epochs using the Optuna framework [ASY$^+$19] to exploit high parallelization and early pruning. In addition to the MLOPT framework in [BS20], we include a specialized solution method for MIQO based on the techniques described in Section 5 where we factorize and cache the factorization of the KKT matrices (8) for each strategy of the problem to speedup the online computations.
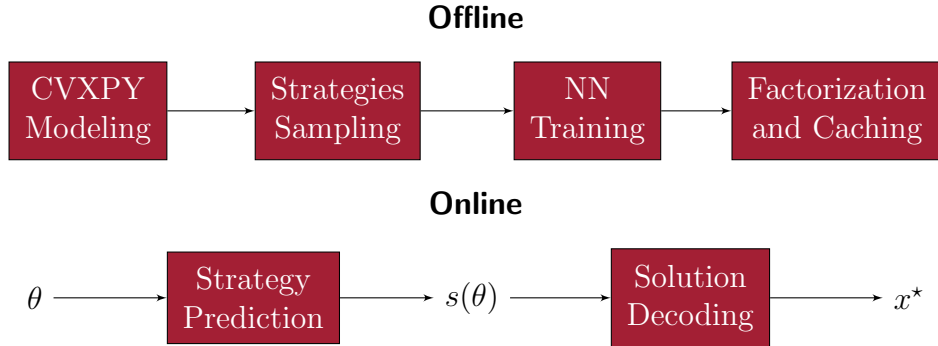
Figure 1: Algorithm implementation

As outlined in Section 5, when we classify online using the NN we pick the best k strategies and evaluate them in parallel, in terms of objective function value and infeasibility, to choose the best one. This step requires a minimal overhead since the matrices are all factorized and we can execute the evaluations in parallel.

We also parallelize the training phase where we collect data and solve the problems over multiple CPUs. The NN training takes place on a GPU which greatly reduces the training time. An overview of the online and offline algorithms appears in Figure 1.

7   Computational Benchmarks

In this section, we benchmark our learning scheme on multiple parametric examples from continuous and mixed-integer problems. We compare the predictive performance and the computational time required by our method to solve the problem compared to using GUROBI Optimizer [GO20]. We run the experiments on the MIT SuperCloud facility in collaboration with the Lincoln Laboratory [RKB$^+$18] exploiting 40 parallel Intel Xeon E5-2650 cores for the data collection involving the problems solution and a NVIDIA Tesla V100 GPU with 16GB for the neural network training. For each problem we sample 100.000 parameters θ_i to collect the strategies. We choose this number because the NN training works better with a large number of data points. Note that, thanks to the multiple cores and the code parallelizations, we were able to train the algorithm between a few hours and less than a day, even for problems that take up to hundreds of seconds to solve with Gurobi.

In addition, for all the examples the Good-Turing estimator condition from Section 4.2 was always satisfied for $\epsilon = 0.001$. We use $10,000$ samples in the test set of the algorithm.

Infeasibility and suboptimality. We follow the same criteria for calculating the relative suboptimality and infeasibility as in [BS20]. We repeat them here for completeness. After the learning phase, we compare the predicted solution $\hat{x}_i^\star$ to the optimal one $x_i^\star$ obtained by solving the instances from scratch. Given a parameter θ_i, we say that the predicted solution is infeasible if the constraints are violated more than $\epsilon_{\text{inf}} = 10^{-4}$ according to the infeasibility metric

$$p(\hat{x}_i^\star) = \|(g(\theta_i, \hat{x}_i^\star))_+\|_\infty / r(\theta_i, \hat{x}_i^\star),$$

where $r(\theta, x)$ normalizes the violation depending on the size of the summands of g. In case of MIQO, $g(\theta, x) = A(\theta)x - b(\theta)$ and $r(\theta, x) = \|b(\theta)\|_\infty$. If the predicted solution $\hat{x}_i$ is feasible, we define its suboptimality as

$$d(\hat{x}_i^\star) = (f(\theta_i, \hat{x}_i^\star) - f(\theta_i, x_i^\star))/|f(\theta_i, x_i^\star)|,$$

where f is the objective of our MIQO problem in (6). Note that $d(\hat{x}_i^\star) \geq 0$ by construction. We consider a predicted solution to be accurate if it is feasible and if the suboptimality is less than the tolerance $\epsilon_{\text{sub}} = 10^{-4}$. For each instance we report the average infeasibility and suboptimality over the samples.

7.1 Fuel Cell Energy Management

Fuel cells are a green highly efficient energy source that need to be controlled to stay within admissible operating ranges. Too large switching between ON and OFF states can reduce both the lifespan of the energy cell and increase energy losses. This is why fuel cells are often paired with energy storage devices such as capacitors which help reducing the switching frequency during fast transients.

In this example we would like to control the energy balance between a super capacitor and a fuel cell in order to match the demanded power [FDM15]. The goal is to minimize the energy losses while maintaining the device within acceptable operating limits to prevent lifespan degradation.

We can model the capacitor dynamics as

$$E_{t+1} = E_t + \tau(P_t - P_t^{\text{load}}), \tag{11}$$

where $\tau > 0$ is the sampling time and $E_t \in [E^{\min}, E^{\max}]$ is the energy stored. $P_t \in [0, P^{\max}]$ is the power provided by the fuel cell and P^{load} is the desired load power.

At each time t we model the on-off state of the fuel cell with the binary variable $z_t \in \{0, 1\}$. When the battery is off $(z_t = 0)$ we do not consume any energy, thus we have $0 \le P_t \le P^{\max} z_t$. When the engine is on $(z_t = 1)$ it consumes $\alpha P_t^2 + \beta P_t + \gamma$ units of fuel, with $\alpha, \beta, \gamma > 0$. We define the stage power cost as

$$f(P, z) = \alpha P^2 + \beta P + \gamma z.$$

We now model the total sum of the switchings over a time window in order to constrain its value. In order to do so we introduce binary variable $d_t \in \{0, 1\}$ determining whether the cell switches at time t either from ON to OFF or viceversa. Additionally we introduce the auxiliary variable $w_t \in [-1, 1]$ accounting for the amount of change brought by d_t in the battery state z_t,

$$w_t = \begin{cases} 1, & d_t = 1 \land z_t = 1, \\ -1, & d_t = 1 \land z_t = 0, \\ 0, & \text{otherwise.} \end{cases} \tag{12}$$

We can model these logical relationships as the following linear inequality [FDM15],

$$G(w_t, z_t, d_t) \le h, \quad \text{with} \quad G = \begin{bmatrix} 1 & 0 & -1 \\ -1 & 0 & -1 \\ 1 & 2 & 2 \\ -1 & -2 & 2 \end{bmatrix}, \quad h = (0, 0, 3, 1). \tag{13}$$

Hence we can write the number of switchings s_{t+1} appeared up to time $t+1$ over the past time window of length T as

$$s_{t+1} = s_t + d_t - d_{t-T}, \tag{14}$$

22

and impose the constraints $s_t \leq n^{\text{sw}}$. The complete fuel cell problem becomes

$$
\begin{aligned}
\text{minimize} \quad & \sum_{t=0}^{T-1} f(P_t, z_t) \\
\text{subject to} \quad & E_{t+1} = E_t + \tau(P_t - P_t^{\text{load}}), \\
& E^{\min} \leq E_t \leq E^{\max}, \\
& 0 \leq P_t \leq z_t P^{\max}, \\
& z_{t+1} = z_t + w_t, \\
& s_{t+1} = s_t + d_t - d_{t-T}, \\
& s_t \leq n^{\text{sw}}, \\
& G(w_t, z_t, d_t) \leq h, \\
& E_0 = E_{\text{init}}, \quad z_0 = z_{\text{init}}, \quad s_0 = s_{\text{init}} \\
& z_t \in \{0, 1\}, \quad d_t \in \{0, 1\}, \quad w \in [-1, 1].
\end{aligned}
\tag{15}
$$

The problem parameters are $\theta = (E_{\text{init}}, z_{\text{init}}, s_{\text{init}}, d^{\text{past}}, P^{\text{load}})$ where $d^{\text{past}} = (d_{-T}, \ldots, d_{-1})$ and $P^{\text{load}} = (P_0^{\text{load}}, \ldots, P_{T-1}^{\text{load}})$. In order to properly control the dynamical system, we must solve (15) within each sampling time τ.

Problem setup. We chose parameters from [FDM15] with values $\alpha = 6.7 \cdot 10^{-4}$, $\beta = 0.2$, $\gamma = 80$ W, and sampling time $\tau = 1$ second We define energy and power constraints with $E^{\min} = 5.2$ kJ, $E^{\max} = 10.2$ kJ and $P^{\max} = 1.2$ kW. The initial values are $E_{\text{init}} = 7.7$ kJ, $z_{\text{init}} = 0$ and $s_{\text{init}} = 0$. We randomly generated the load profile P^{load}.

   We obtain the offline samples by simulating a closed-loop trajectory of $10,000$ time steps and storing the parameters for each component of θ along the trajectory *i.e.*, $E_{\text{init}}, z_{\text{init}}, s_{\text{init}}, d^{\text{past}}$, and P^{load}. We, then, sample from a uniform distribution over a hypershpere of radius 0.5 centered at each trajectory point. Afterwards, we enforce the feasibility of the problem parameters according to the constraints in (15).

Results. Table 1 reports the problem dimensions and the maximum computation time needed with each technique. Figure 2 shows the performance of MLOPT for varying values of the top-k strategies and in terms of computation time, suboptimality, infeasibility and accuracy. As expected, as k increases the performance improves. For time horizons of $T = 50$ or $T = 60$, Gurobi takes on average longer than the allowed sampling time, $\tau = 1$ sec. As noted by the authors of [FDM15], in order to get good performance with
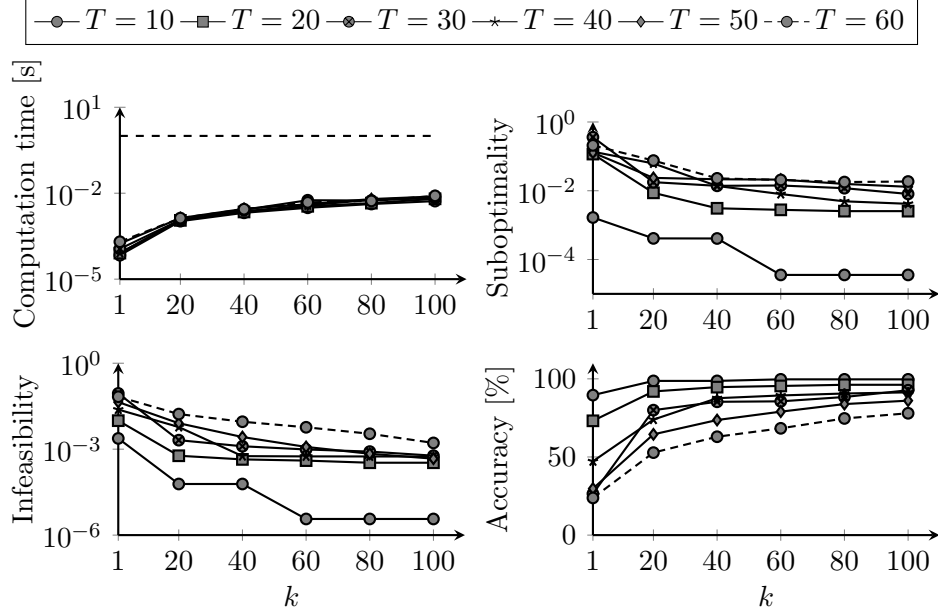
23

Figure 2: MLOPT average performance indicators for fuel cell battery management example. The dashed line indicates the sampling time.

this system, horizons in at least of $T = 60$ need to be considered and the respective solutions are not computable in less than $\tau = 1$ sec with state-of-the-art algorithms. From Table 1, the maximum time of Gurobi is above the allowed sampling time for horizons ≥ 20 and Gurobi heuristic for horizon ≥ 40. Therefore, these solution methods are not applicable for real-time optimization of this dynamical systems.

7.2 Portfolio Trading

Consider the portfolio investment problem [Mar52, BBD$^+$17]. This problem has been extensively analyzed in robust optimization [BP08] and stochastic control settings [HDG07]. The decision variables are the normalized portfolio weights $w_t \in \mathbf{R}^{n+1}$ at time t corresponding to each of the assets in the portfolio and a riskless asset at the $(n + 1)$-th position denoting a cash account. We define the trade as the difference of consecutive weights $w_t - w_{t-1}$ where w_{t-1} is the given vector of current asset investments acting as a problem
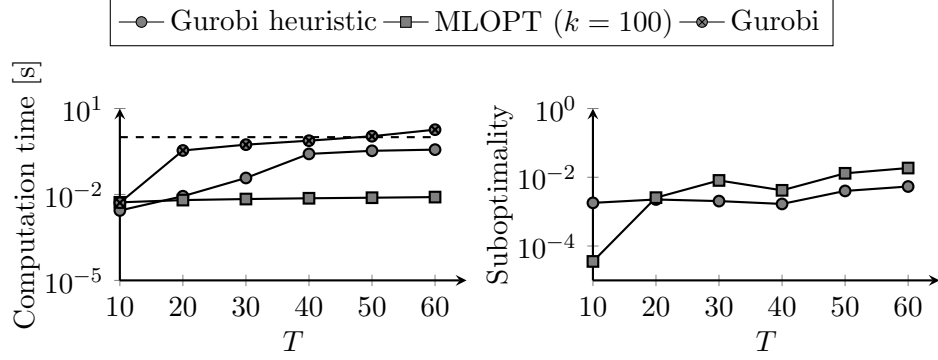
Figure 3: Comparison between Gurobi and MLOPT performance for the fuel cell battery management example. Average computation time and suboptimality. The dashed line indicates the sampling time.

Table 1: Fuel cell energy management problem dimensions and maximum times.

T	n_{var}	n_{constr}	M	t_{max} MLOPT [s]	t_{max} Gurobi [s]	t_{max} Gurobi heuristic [s]
10	88	207	709	0.1402	0.0875	0.0076
20	178	417	1863	0.1834	1.3175	0.0370
30	268	627	4119	0.2410	1.4870	0.3108
40	358	837	1720	0.2354	2.1782	1.1928
50	448	1047	8133	0.1673	5.8576	1.4715
60	538	1257	9200	0.2486	10.8647	1.8297

parameter. The goal is to maximize the risk-adjusted returns as follows

$$
\begin{aligned}
\text{maximize} \quad & \hat{r}_t^T w_t - \gamma \ell_t^{\text{risk}}(w_t) - \ell_t^{\text{hold}}(w_t) - \ell_t^{\text{trade}}(w_t - w_{t-1}) \\
\text{subject to} \quad & \mathbf{1}^T w_t = 1, \\
& \mathbf{card}(w_t) \leq c.
\end{aligned}
\tag{16}
$$

Four terms compose the stage rewards. First, we describe returns $\hat{r}_t^T w_t$ as a function of the estimated stock returns $\hat{r}_t \in [0,1]^{n+1}$ at time t. Second, we define the risk cost as

$$
\ell_t^{\text{risk}}(x) = x^T \hat{\Sigma}_t x,
$$

where $\hat{\Sigma}_t \in \mathbf{S}_+^{(n+1)\times(n+1)}$ is the estimate of the covariance of the returns at time t. Third, we define the holding cost as

$$
\ell_t^{\text{hold}}(x) = s_t^T(x)_-,
$$

where $(s_t)_i \geq 0$ is the borrowing fee for shorting asset i at time t. The fourth term describes a penalty on the trades defined as

$$
\ell_t^{\text{trade}}(x) = \lambda \|x_t - x_{t-1}\|_1,
$$

Parameter $\lambda > 0$ denotes the relative cost importance of penalizing the trades. The first constraint enforces the portfolio weights normalization while the second constraints the maximum number of nonzero asset investments, i.e., the cardinality, to be less than $c \in \mathbf{Z}_{>0}$. For the complete model derivation without cardinality constraints see [BBD+17, Section 5.2].

Risk model. We use a common risk model described as a k-factor model $\Sigma_t = F_t \Sigma_t^F F_t^T + D_t$ where $F_t \in \mathbf{R}^{(n+1)\times k}$ is the factor loading matrix and $\Sigma_t^F \in \mathbf{S}_+^{k\times k}$ is an estimate of the factor returns $F^T r_t$ covariance [BBD+17]. Each entry $(F_t)_{ij}$ is the loading of asset i to factor j. $D_t \in \mathbf{S}_+^{(n+1)\times(n+1)}$ is a nonnegative diagonal matrix accounting for the additional variance in the asset returns usually called idiosyncratic risk. We compute the factor model estimates $\hat{\Sigma}_t$ with 15 factors by using a similar method as in [BBD+17, Section 7.3] where we take into account data from the two years time window before time t.

Return forecasts. In practice return forecasts are always proprietary and come from sophisticated prediction techniques based on a wide variety of data available to the trading companies. In this example, we simply add zero-mean noise to the realized returns to obtain the estimates and then rescale them to have a realistic mean square error of our prediction. While these estimates are not real because they use the actual returns, they provide realistic values for the purpose of our computations. We assume to know the risk-free interest rates exactly with $(\hat{r}_t)_{n+1} = (r_t)_{n+1}$. The return estimates for the non-cash assets are $(\hat{r}_t)_{1:n} = \alpha((r_t)_{1:n} + \epsilon_t)$ where $\epsilon_t \sim \mathcal{N}(0, \sigma_\epsilon I)$ and $\alpha > 0$ is the scaling to minimize the mean-squared error $\mathbf{E}((\hat{r}_t)_{1:n} - (r_t)_{1:n})^2$ [BBD+17, Section 7.3]. This method gives us return forecasts in the order of $\pm 0.3\%$ with an information ratio $\sqrt{\alpha} \approx 0.15$ typical of a proprietary return forecast prediction.

Parameters. The problem parameters are $\theta = (w_{t-1}, r_t, D_t, \Sigma_t^F, F_t)$ which, respectively, correspond to the previous assets allocation, vector of returns and the risk model matrices. Note that the risk model is updated at the beginning of every month. Since the parameters not only affect the data in problem vectors, but also in the matrices, we cannot exploit the offline factorization caching for linear system (8).

Problem setup. We simulate the trading system using the S&P100 values [Qua19] from 2008 to 2013 with risk cost $\gamma = 100$, borrow cost $s_t = 0.0001$ and trade cost $\lambda = 0.01$. These values are similar as the benchmark values in [BBD+17]. We use different sparsity levels c from 1 to 40. Afterwards we collect data by sampling around the trajectory points from a hypersphere with radius 0.001 times the magnitude of the parameter. For example, for a vector of returns of magnitude $\bar{r}_t$ we sample around r_t with a radius $0.001\bar{r}_t$. Even though this problem does not have to be solved in real-time, in order to optimize the trading performance, we must perform multiple expensive backtesting simulations.

Results. Table 2 shows the problem dimensions and the maximum computation time needed with each technique. Figure 4 displays the performance of MLOPT for varying values of the top-k strategies and in terms of computation time, suboptimality, infeasibility and accuracy. For smaller c, although the total number of integer variable combinations is lower, the problem is
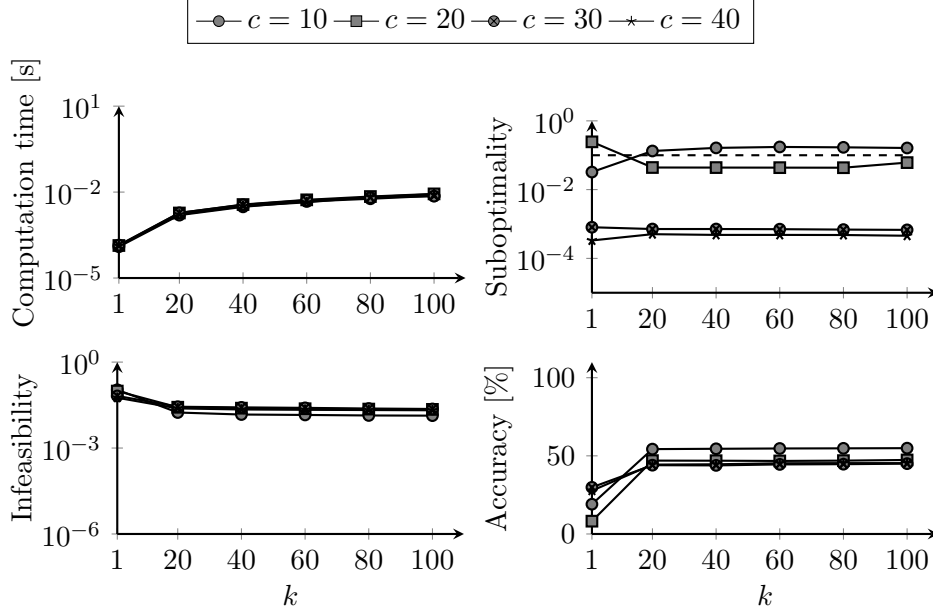
Figure 4: MLOPT average performance indicators for portfolio example.

harder to solve for every technique. In this example, the performance does not significantly increase above $k = 20$. We suspect that further accuracy improvements should happen with $k > 100$. In addition, suboptimality is very low for $c = 30$ and $c = 40$. The performance comparison between the different methods appears in Figure 5. MLOPT shows up to three orders of magnitude speedups over Gurobi and Gurobi heuristic despite moderate suboptimality and infeasibility values, mostly for $c = 10$ and $c = 20$. With these computation time speedups, backtesting time can be significantly reduced and multiple parameter simulations can be executed to tune the problem parameters while evaluating the performance on historical data. This is crucial to obtain high quality portfolio trades.

7.3 Motion Planning

We consider the problem of motion planning in the presence of obstacles. This problem has a wide variety of applications including autonomous vehicles, space robots, and unmanned aerial vehicless (UAVs) [LaV06]. These problems must usually be solved online within a few milliseconds to provide
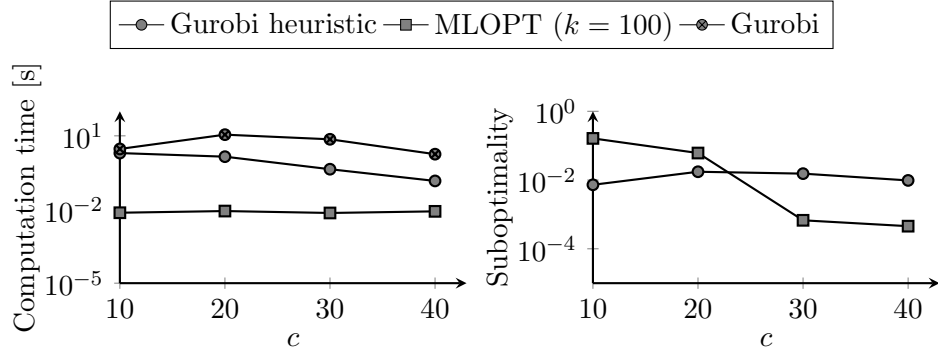
Figure 5: Comparison between Gurobi and MLOPT performance for the portfolio example. Average computation time and suboptimality. The dashed line indicates the sampling time.

Table 2: Portfolio problem dimensions and maximum times.

c	n_{var}	n_{constr}	M	$t_{\max}$ MLOPT [s]	$t_{\max}$ Gurobi [s]	$t_{\max}$ Gurobi heuristic [s]
10	552	902	4153	0.1507	45.7616	28.8303
20	552	902	3009	0.1754	2063.7874	62.3858
30	552	902	3317	0.1998	479.8125	4.6310
40	552	902	3722	0.0967	222.6169	2.5596

inputs that are frequent enough to control the system dynamics. Unfortunately, the presence of obstacles makes the problem nonconvex and, therefore, very challenging to solve online. In the literature, several approaches have been proposed to model the motion planning problem with MIO [SDFH01]. However, solution times in the order of a few milliseconds are still out of reach of state-of-the-art MIO solvers.

We consider the problem in d dimensions, in practice $d = 2$ for planar systems or $d = 3$ for aerial systems. The state of the system is $x_t = (p_t, v_t)$ where $p_t \in \mathbf{R}^d$ is the position at time t and $v_t \in \mathbf{R}^d$ the velocity. The input $u_t \in \mathbf{R}^d$ are the forces produced by the system in every direction. For example, for an UAV, u_t corresponds to the thruster forces. The discrete-time linear system dynamics are described as

$$(p_{t+1}, v_{t+1}) = A(p_t, v_t) + Bu_t, \qquad t = 0, \ldots, T,$$

where $A \in \mathbf{R}^{2d \times 2d}$ and $B \in \mathbf{R}^{2d \times d}$ and $\tau > 0$ is the sampling time. The initial state of the system is $(p^{\text{init}}, v^{\text{init}})$. We define upper and lower bounds on the state and inputs as

$$\underline{p} \leq p_t \leq \overline{p}, \qquad \underline{v} \leq v_t \leq \overline{v}, \qquad t = 0, \ldots, T,$$
$$\underline{u} \leq u_t \leq \overline{u}, \qquad t = 0, \ldots, T-1.$$

We model every obstacle i as a rectangle in $\mathbf{R}^d$ with upper bounds $\overline{o}^i \in \mathbf{R}^d$ and lower bounds $\underline{o}^i \in \mathbf{R}^d$ for $i = 1, \ldots, n_{\text{obs}}$. At every time t and for every obstacle i, we model the obstacle avoidance decisions with binary variables $\overline{\delta}_t^i \in \{0, 1\}^d$ for the obstacle upper bounds and $\underline{\delta}_t^i \in \{0, 1\}^d$ for the lower bounds. We can write obstacle avoidance as the following big-M conditions

$$\overline{o}^i - M\overline{\delta}_t^i \leq p_t \leq \underline{o}^i + M\underline{\delta}_t^i, \qquad t = 0, \ldots, T, \quad i = 1, \ldots, n_{\text{obs}}.$$

In addition, we must impose that we cannot be at the same time on different sides of an obstacle,

$$\mathbf{1}^T \underline{\delta}_t^i + \mathbf{1}^T \overline{\delta}_t^i \leq 2d - 1, \qquad t = 0, \ldots, T, \quad i = 1, \ldots, n_{\text{obs}},$$

where $\mathbf{1}$ is the vector of ones of dimension d. Our goal is to minimize the distance with respect to a desired position ($p_t \approx p^{\text{des}}$) while expending minimal control effort ($u_t \approx 0$). We can write the cost as

$$\|p_T - p^{\text{des}}\|_2^2 + \sum_{t=0}^{T-1} \|p_t - p^{\text{des}}\|_2^2 + \gamma \|u_t\|_2^2,$$

where $\gamma > 0$ balances the trade-off between performance and control effort. The motion planning problem can be written as

$$
\begin{aligned}
\text{minimize} \quad & \|p_T - p^{\text{des}}\|_2^2 + \sum_{t=0}^{T-1} \|p_t - p^{\text{des}}\|_2^2 + \gamma \|u_t\|_2^2 \\
\text{subject to} \quad & (p_{t+1}, v_{t+1}) = A(p_t, v_t) + B u_t, \qquad t = 0, \dots, T-1 \\
& p_0 = p^{\text{init}}, \quad v_0 = v^{\text{init}} \\
& \bar{o}^i - M\bar{\delta}_t^i \leq p_t \leq \underline{o}^i + M\underline{\delta}_t^i, \qquad t = 0, \dots, T, \quad i = 1, \dots, n_{\text{obs}} \\
& \mathbf{1}^T \underline{\delta}_t^i + \mathbf{1}^T \bar{\delta}_t^i \leq 2d - 1 \qquad t = 0, \dots, T \\
& \bar{\delta}_t^i \in \{0,1\}^d, \quad \underline{\delta}_t^i \in \{0,1\}^d, \qquad i = 1, \dots, n_{\text{obs}} \\
& x_t \in [\underline{x}, \bar{x}], \qquad t = 0, \dots, T, \\
& u_t \in [\underline{u}, \bar{u}], \qquad t = 0, \dots, T-1.
\end{aligned}
\tag{17}
$$

Parameters. We consider the problem of computing the optimal trajectory from any point in the plane to the desired position p^{des}. In this example the rest of the problem data does not change. Therefore, the problem parameters are the initial state $\theta = p^{\text{init}}$. Problem (17) must be solved within each sampling time τ to provide fast enough inputs to the dynamical system.

Problem setup. We consider a discrete-time double-integrator dynamical system in two dimensions as in [SDFH01]. The optimizer must provide solutions within the sampling time 0.1 sec in order to operate the system properly. The time horizon is $T = 60$ which corresponds to 6 sec. The cost tradeoff parameter is $\gamma = 0.01$. The initial state is given by $p^{\text{init}} = \theta$ and $v^{\text{init}} = 0$. The desired position is $p^{\text{des}} = (-10.5, -10)$ and the desired velocity $v^{\text{des}} = 0$. Figure 6 shows an example trajectory for $\theta = (9, 13)$. To generate training samples θ_i, we sample uniformly between $\underline{p}$ and $\bar{p}$.

Results. Table 3 shows the problem dimensions along with the maximum computation time taken by each technique. Figure 4 shows the average performance of MLOPT for varying top-k strategies selected. Even if the accuracy is always low, most of the times less than 10%, the suboptimality and infeasibility are acceptable for this application. As shown in Figure 6, there can be some constraints violations due to marginal violations of the obstacle boundaries. We show the direct comparison of Gurobi, Gurobi heuristic and
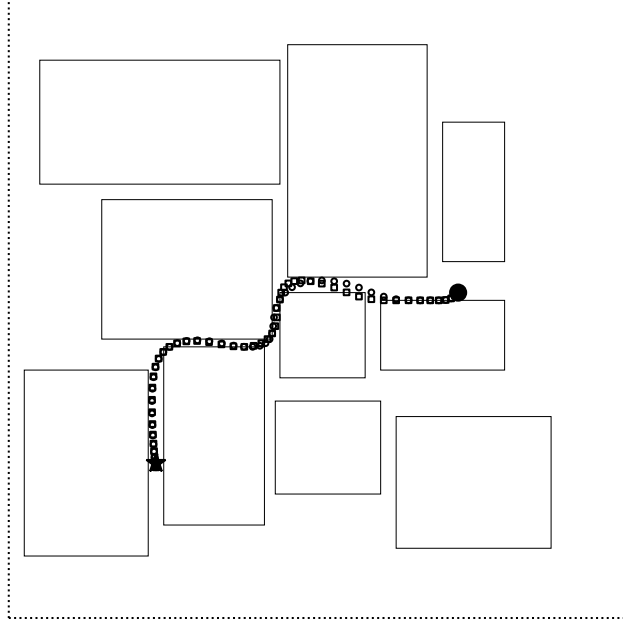
Figure 6: Trajectory planning example with 10 obstacles and sampling time 0.1 sec. Circles indicate the optimal path computed with Gurobi in 18.18 sec and the squares indicate the optimal path computed with MLOPT with $k = 100$ in 0.06 sec. The filled dot is the starting position while the start is the desired position. The boundaries of the feasible positions are the dotted line while obstaces are displayed as rectangles.

MLOPT in Figure 8. The time improvements of MLOPT allow its real-time implementation, in contrast to state-of-the-art options.

7.4 Remarks

The numerical examples show several benefits of our approach. First, the strategy pruning technique allows us to work with a total number of strategies between 100 and 10,000. These numbers allow high quality predictions in terms of suboptimality and infeasibility with NNs combined with top-k strategies selection. Second, despite low accuracy when comparing the predicted strategy to the exact optimal one, the average subptimality is com-
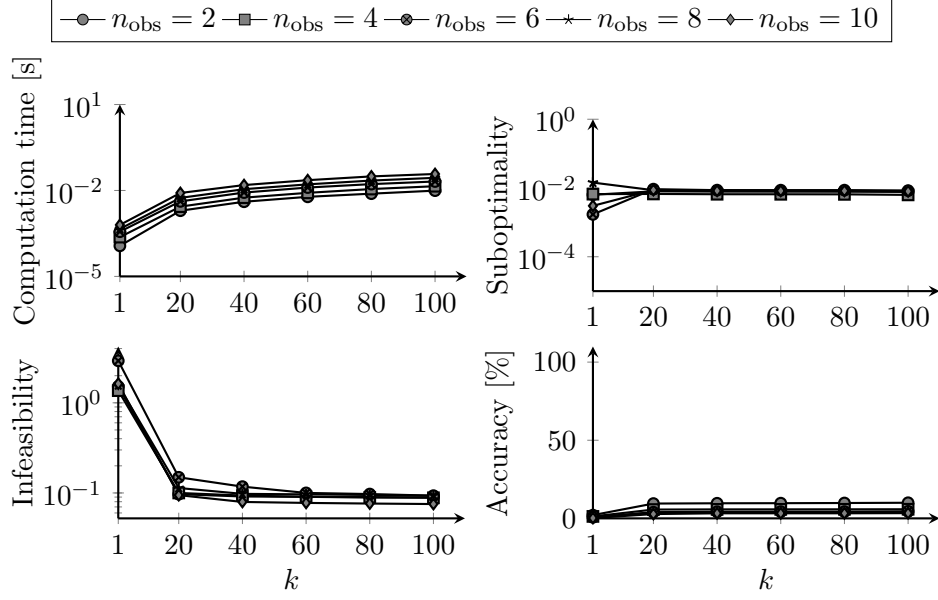
Figure 7: MLOPT average performance indicators for motion planning example. The dashed line indicates the sampling time.
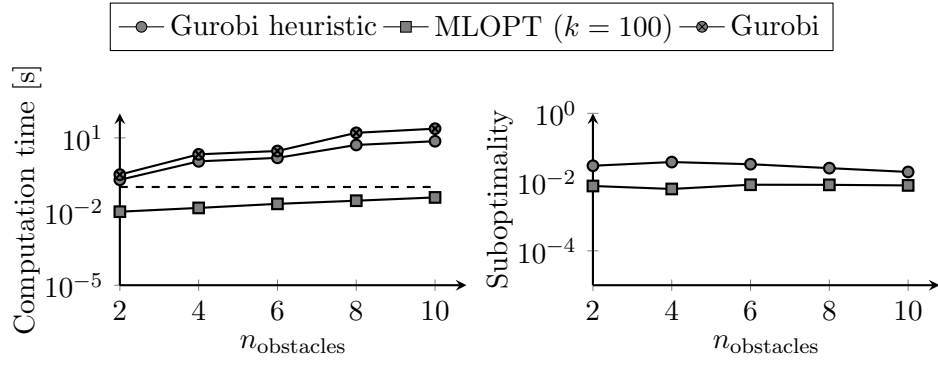

Figure 8: Comparison between Gurobi and MLOPT performance for the motion planning example. Average computation time and suboptimality. The dashed line indicates the sampling time.

Table 3: Motion planning problem dimensions and maximum times.

$n_{\text{obstacles}}$	n_{var}	n_{constr}	M	$t_{\max}$ MLOPT [s]	$t_{\max}$ Gurobi [s]	$t_{\max}$ Gurobi heuristic [s]
2	1135	3773	1371	0.4145	2.3776	2.2962
4	1615	10133	1135	0.1878	11.8172	8.1443
6	2095	20333	939	0.3173	33.7869	11.5292
8	2575	34373	845	0.2235	392.3073	128.4948
10	3055	52253	696	0.2896	773.1476	206.4520

parable or better than the one of Gurobi heuristic. In addition, infeasibility is always within acceptable levels for the proposed application. This means that, even in case of multiple global minimizers, our method is able to consistently predict optimal or close-to-optimal solutions. Third, time measurements show up to three orders of magnitude speedups of MLOPT compared to Gurobi and Gurobi heuristics, both in terms of average and worst-case solution time. Since for the fuel cell energy management and the motion planning examples, optimal solutions must be computed within hard real-time requirements, only fast optimization methods can be implemented in practice and Gurobi-based approaches are too slow. On the contrary, MLOPT proves to be a much faster approach for computing online solutions.

8   Conclusions

We proposed a machine learning method for solving online MIO at very high speed. By using the Voice of Optimization framework [BS20] we exploited the repetitive nature of online optimization problems to greatly reduce the solution time. Our method casts the core part of the optimization algorithm as a multiclass classification problem that we solve using a NN. In this work we considered the class of MIQO which, while covering the vast majority of real-world optimization problems, allows us to further reduce the computation time exploiting its structure. For MIQO, we only have to solve a linear system to obtain the optimal solution after the NN prediction. In other words, our approach does not require any solver nor iterative routine to solve parametric MIQOs. Our method is not only extremely fast but also reliable. Compared to branch-and-bound methods our approach has a very predictable online solution time for which we can exactly bound

the flops complexity. This is of crucial importance for real-time applications. We benchmarked our approach against the state-of-the-art solver Gurobi on different real-world examples showing 100 to 1000 fold speedups in online execution time.

There are several future research directions to improve the MLOPT framework. First, specialized neural networks architectures might provide more accurate strategy classifiers for optimization problems with a specific structure. Second, the MLOPT training phase at the moment requires computing the optimal solution of problems with several different parameter combinations. Therefore, the current approach does not apply to problems that take hours to solve with Gurobi. Using suboptimal solutions in the training phase would allow us significantly reduce the training time and apply MLOPT to such problems. Third, strategy reduction techniques combined with structure exploiting classifiers would enable applications to large-scale optimization problems with only discrete variables. Finally, including the knowledge about the previous solution would improve the performance of MLOPT, similarly to how warm-starting techniques help reducing computations in MIO solvers.

Acknowledgment

References

[AAB+19]   A. Agrawal, B. Amos, S. Barratt, S. Boyd, S. Diamond, and Z. Kolter. Differentiable convex optimization layers. In *Advances in Neural Information Processing Systems*, 2019.

[ALW17]   A. M. Alvarez, Q. Louveaux, and L. Wehenkel. A machine learning-based approximation of strong branching. *INFORMS Journal on Computing*, 29(1):185–195, 2017.

[ASY+19]   Takuya Akiba, Shotaro Sano, Toshihiko Yanase, Takeru Ohta, and Masanori Koyama. Optuna: A next-generation hyperpa-

rameter optimization framework. In *Proceedings of the 25rd ACM SIGKDD International Conference on Knowledge Discovery and Data Mining*, 2019.

[BBD+17]   S. Boyd, E. Busseti, S. Diamond, R. N. Kahn, K. Koh, P. Nystrup, and J. Speth. Multi-period trading via convex optimization. *Foundations and Trends in Optimization*, 3(1):1–76, 2017.

[BDTD+16]   M. Bojarski, D. Del Testa, D. Dworakowski, B. Firner, B. Flepp, P. Goyal, L. D. Jackel, M. Monfort, U. Muller, J. Zhang, X. Zhang, J. Zhao, and K. Zieba. End to end learning for self-driving cars. arXiv:1604.07316, 2016.

[Bix10]   R. E. Bixby. A brief history of linear and mixed-integer programming computation. *Documenta Mathematica*, pages 107–121, 2010.

[BLP18]   Y. Bengio, A. Lodi, and A. Prouvost. Machine learning for combinatorial optimization: a methodological tour d'horizon. arXiv:1811.0612, 2018.

[BLZ18]   P. Bonami, A. Lodi, and G. Zarpellon. Learning a classification of mixed-integer quadratic programming problems. In Willem-Jan van Hoeve, editor, *Integration of Constraint Programming, Artificial Intelligence, and Operations Research*, pages 595–604, Cham, 2018. Springer International Publishing.

[BM99]   A. Bemporad and M. Morari. Control of systems integrating logic, dynamics, and constraints. *Automatica*, 35(3):407–427, 1999.

[BMDP02]   A. Bemporad, M. Morari, V. Dua, and E. N. Pistikopoulos. The explicit linear quadratic regulator for constrained systems. *Automatica*, 38(1):3–20, 2002.

[BP08]   D. Bertsimas and D. Pachamanova. Robust multiperiod portfolio management in the presence of transaction costs. *Computers & Operations Research*, 35(1):3 – 17, 2008.

[BS20]   D. Bertsimas and B. Stellato. The Voice of Optimization. *Machine Learning (to appear)*, 2020.

[BSM+17]   G. Banjac, B. Stellato, N. Moehle, P. Goulart, A. Bemporad, and S. Boyd. Embedded code generation using the OSQP solver. In *IEEE Conference on Decision and Control (CDC)*, 2017.

[BT97]   D. Bertsimas and J. N. Tsitsiklis. *Introduction to Linear Optimization.* Athena Scientific, 1997.

[BV04]   S. Boyd and L. Vandenberghe. *Convex Optimization.* Cambridge University Press, 2004.

[BW05]   D. Bertsimas and R. Weismantel. *Optimization Over Integers.* Dynamic Ideas Press, 2005.

[CaPM10]   J. P. S Catalão, H.M.I. Pousinho, and V.M.F. Mendes. Scheduling of head-dependent cascaded hydro systems: Mixed-integer quadratic programming approach. *Energy Conversion and Management*, 51(3):524 – 530, 2010.

[CCS+20]   A. Cauligi, P. Culbertson, B. Stellato, D. Bertsimas, M. Schwager, and M. Pavone. Learning mixed-integer convex optimization strategies for robot planning and control, 2020.

[Dav06]   T. A. Davis. *Direct Methods for Sparse Linear Systems.* Society for Industrial and Applied Mathematics, 2006.

[DB16]   S. Diamond and S. Boyd. CVXPY: A Python-embedded modeling language for convex optimization. *Journal of Machine Learning Research*, 17(83):1–5, 2016.

[DCB00]   O. Damen, A. Chkeif, and Belfiore. Lattice code decoder for space-time codes. *IEEE Communications Letters*, 4(5):161–163, May 2000.

[DCB13]   A. Domahidi, E. Chu, and S. Boyd. ECOS: An SOCP solver for embedded systems. In *European Control Conference (ECC)*, pages 3071–3076, 2013.

[DDS16]   H. Dai, B. Dai, and L. Song. Discriminative embeddings of latent variable models for structured data. In *Proceedings of the 33rd International Conference on International Conference on Machine Learning - Volume 48*, ICML'16, pages 2702–2711. JMLR.org, 2016.

[DKZ+17]   H. Dai, E. B. Khalil, Y. Zhang, B. Dilkina, and L. Song. Learning combinatorial optimization algorithms over graphs. arXiv:1704.01665, 2017.

[DTB18]   S. Diamond, R. Takapoui, and S. Boyd. A general system for heuristic minimization of convex functions over non-convex sets. *Optimization Methods and Software*, 33(1):165–193, 2018.

[Fal19]   WA Falcon. Pytorch lightning. github.com/PyTorchLightning/pytorch-lightning, 2019.

[FDM15]   D. Frick, A. Domahidi, and M. Morari. Embedded optimization for mixed logical dynamical systems. *Computers & Chemical Engineering*, 72:21–33, 2015.

[FGL05]   M. Fischetti, F. Glover, and A. Lodi. The feasibility pump. *Mathematical Programming*, 104(1):91–104, 2005.

[FKP+14]   H. J. Ferreau, C. Kirches, A. Potschka, H. G. Bock, and M. Diehl. qpOASES: a parametric active-set algorithm for quadratic programming. *Mathematical Programming Computation*, 6(4):327–363, 2014.

[GBC16]   I. Goodfellow, Y. Bengio, and A. Courville. *Deep Learning*. MIT Press, 2016.

[GHW15]   G. Gamrath, B. Hiller, and J. Witzig. Reoptimization techniques for MIP solvers. In E. Bampis, editor, *Experimental Algorithms*, pages 181–192. Springer International Publishing, 2015.

[GO20]   LLC Gurobi Optimization. Gurobi optimizer reference manual, 2020.

[Goo53]   I. J. Good. The population frequencies of species and the estimation of population parameters. *Biometrika*, 40(3/4):237–264, 1953.

[HDG07]   F. Herzog, G. Dondi, and H. P. Geering. Stochastic model predictive control and portfolio optimization. *International Journal of Theoretical and Applied Finance (IJTAF)*, 10(02):203–233, 2007.

[HDY+12]   G. Hinton, L. Deng, D. Yu, G. E. Dahl, A. Mohamed, N. Jaitly, A. Senior, V. Vanhoucke, P. Nguyen, T. N. Sainath, and B. Kingsbury. Deep neural networks for acoustic modeling in speech recognition: The shared views of four research groups. *IEEE Signal Processing Magazine*, 29(6):82–97, Nov 2012.

[HR14]   A. Hassanzadeh and T. K. Ralph. On the value function of a mixed integer linear optimization problem and an algorithm for its construction. Technical report, COR@L Laboratory Report 14T-004, Lehigh University, 2014.

[JLN+10]   M. Jünger, T. M. Liebling, D. Naddef, G. L. Nemhauser, W. R. Pulleyblank, G. Reinelt, G. Rinaldi, and L. A. Wolsey. *50 Years of Integer Programming 1958-2008*. Springer Berlin Heidelberg, 2010.

[KBS+16]   E. B. Khalil, P. L. Bodic, L. Song, G. Nemhauser, and B. Dilkina. Learning to branch in mixed integer programming. In *Proceedings of the Thirtieth AAAI Conference on Artificial Intelligence*, AAAI'16, pages 724–731. AAAI Press, 2016.

[KKK19]   M. Klaučo, M. Kalúz, and M. Kvasnica. Machine learning-based warm starting of active set methods in embedded model predictive control. *Engineering Applications of Artificial Intelligence*, 77:1 – 8, 2019.

[KSH12]   A. Krizhevsky, I. Sutskever, and G. E. Hinton. Imagenet classification with deep convolutional neural networks. In *Advances in Neural Information Processing Systems*, page 2012, 2012.

[LaV06]   Steven M. LaValle. *Planning Algorithms*. Cambridge University Press, USA, 2006.

[LBH15]   Y. LeCun, Y. Bengio, and G. Hinton. Deep learning. *Nature*, 521(7553):436–444, may 2015.

[LZ17]   A. Lodi and G. Zarpellon. On learning and branching: a survey. *TOP*, 25(2):207–236, Jul 2017.

[Mar52]   H. Markowitz. Portfolio selection. *The Journal of Finance*, 7(1):77–91, 1952.

[MB12]   J. Mattingley and S. Boyd. CVXGEN: A code generator for embedded convex optimization. *Optimization and Engineering*, 13(1):1–27, 2012.

[MRN19]   S. Misra, L. Roald, and Y. Ng. Learning for constrained optimization: Identifying optimal active constraint sets. arXiv:1802.09639, 2019.

[MT19]   Tobia Marcucci and Russ Tedrake. Warm start of mixed-integer programs for model predictive control of hybrid systems. arXiv:1910.08251, 2019.

[NW06]   J. Nocedal and S. J. Wright. *Numerical Optimization*. Springer Series in Operations Research and Financial Engineering. Springer, Berlin, 2nd edition, 2006.

[PGC+17]   A. Paszke, S. Gross, S. Chintala, G. Chanan, E. Yang, Z. De-Vito, Z. Lin, A. Desmaison, L. Antiga, and A. Lerer. Automatic differentiation in PyTorch. In *NIPS-W*, 2017.

[PS82]   C. C. Paige and M. A. Saunders. LSQR: An algorithm for sparse linear equations and sparse least squares. *ACM Trans. Math. Softw.*, 8(1):43–71, March 1982.

[Qua19]   Quandl. WIKI S&P100 End-Of-Day Data, 2019.

[RG06]   T. L. Ralphs and M. Güzelsoy. Duality and warm starting in integer programming. In *The Proceedings of the 2006 NSF Design, Service, and Manufacturing Grantees and Research Conference*, 2006.

[RKB+18]   A. Reuther, J. Kepner, C. Byun, S. Samsi, W. Arcand, D. Bestor, B. Bergeron, V. Gadepally, M. Houle, M. Hubbell, M. Jones, A. Klein, L. Milechin, J. Mullen, A. Prout, A. Rosa, C. Yee, and P. Michaleas. Interactive supercomputing on 40,000 cores for machine learning and data analysis. In *2018 IEEE High Performance extreme Computing Conference (HPEC)*, pages 1–6, Sep. 2018.

[SB18]   R. S. Sutton and A. G. Barto. *Reinforcement Learning: An Introduction*. A Bradford Book, 2nd edition, 2018.

[SBG+20]   B. Stellato, G. Banjac, P. Goulart, A. Bemporad, and S. Boyd. OSQP: An Operator Splitting Solver for Quadratic Programs, feb 2020.

[SDFH01]   T. Schouwenaars, B. De Moor, E. Feron, and J. How. Mixed integer programming for multi-vehicle path planning. In *2001 European Control Conference (ECC)*, pages 2603–2608, 2001.

[SSS+17]   D. Silver, J. Schrittwieser, K. Simonyan, I. Antonoglou, A. Huang, A. Guez, T. Hubert, L. Baker, M. Lai, A. Bolton, Y. Chen, L. Lillicrap, F. Hui, L. Sifre, G. van den Driessche, T. Graepel, and D. Hassabis. Mastering the game of go without human knowledge. *Nature*, 550(7676):354–359, oct 2017.

[TPS13]   A. C. Trapp, O. A. Prokopyev, and A. J. Schaefer. On a level-set characterization of the value function of an integer program and its application to stochastic programming. *Operations Research*, 61(2):498–511, 2013.

[TPS19]   O. Tavasloğlu, O. A. Prokopyev, and A. J. Schaefer. Solving stochastic and bilevel mixed-integer programs via a generalized value function. *Operations Research*, 67(6):1659–1677, 2019.

[YG08]   F. You and I. E. Grossmann. Mixed-integer nonlinear programming models and algorithms for large-scale supply chain design with stochastic inventory management. *Industrial & Engineering Chemistry Research*, 47(20):7802–7817, 2008.